MICROSTRUCTURE AND MECHANICAL PROPERTIES AT ELEVATED TEMPERATURES OF POLYCRYSTALLINE Al_2O_3-YAG-ZrO_2 EUTECTIC-COMPOSITION COMPOSITES

F.A. Huamán-Mamani, M. Jiménez-Melendo*

Departamento de Física de la Materia Condensada and Instituto de Ciencia de Materiales (CSIC-Universidad de Sevilla). Aptdo. 1065. 41080 Sevilla, Spain
**melendo@us.es*

Keywords: alumina, YAG, zirconia, creep

Abstract
The microstructural and high-temperature mechanical characteristics of conventionally sintered Al_2O_3-$Y_3Al_5O_{12}$-ZrO_2 polycrystals with the ternary eutectic composition have been investigated. An equiaxed and fine-grained microstructure was obtained after the sintering of commercial powders of Al_2O_3, Y_2O_3 and ZrO_2 at 1500 ºC for 10 h in air. The mechanical behavior was assessed by compression testing at constant strain rate and at constant load in air at temperatures between 1200 and 1400 ºC. A brittle to ductile transition was observed with increasing temperature. Grain boundary sliding is the primary deformation mechanism in the ductile regime, as found in fine-grained superplastic metals and ceramics.

1 Introduction

Directionally solidified eutectic oxide composites grown from the melt through a controlled system have received much attention in the last two decades because of their excellent mechanical properties even at temperatures close to the eutectic temperature [1-5]. These properties derive from the lamellar microstructure obtained during solidification which minimizes the free energy at the interfaces, resulting in single crystal phases entangled with each other. In particular, directionally solidified Al_2O_3-based eutectic oxide composites (such as Al_2O_3-YAG, Al_2O_3-ZrO_2, Al_2O_3-$GdAlO_3$, etc.) have been intensively studied as potential candidates for high-temperature section components in important fields including aerospace, aeronautics and high-efficiency power generation systems. At room temperature, a fracture toughness as high as 8 MPa.$m^{1/2}$ has been reported in the ternary Al_2O_3-YAG-ZrO_2 eutectic [5]. A flexural strength of 2 GPa was also reported in the binary Al_2O_3-YAG eutectic composite [2]. At elevated temperatures, the most remarkable property is the retention of large flexural, tensile and compressive strengths up to temperatures close to the eutectic temperature [1].

In contrast, the processing routes necessary to produce directionally solidified eutectic ceramics are expensive and do not allow for the fabrication of large and custom-shaped component parts. Polycrystalline Al_2O_3-based composites have been largely investigated in the past because they exhibit improved properties relative to their single-phase constituents. For example, dual phase Al_2O_3-ZrO_2 composites (ZTA) show enhanced fracture resistance and strength [6]. They also exhibit a remarkable resistance to coarsening at elevated temperatures, which has been exploited to achieve superplasticity [7]. Moreover, garnet-structure oxides are also very attractive candidates for high-temperature structural

applications because of their excellent creep strength; among these oxides, yttrium aluminum garnet $Y_3Al_5O_{12}$ (YAG) has the highest melting temperature and is fairly stable in oxidizing and reducing atmospheres [8]. Very few studies are concerned with Al_2O_3-YAG-ZrO_2 polycrystals; and to our knowledge, only one work has focused on their mechanical behavior at room temperature [9]. The mechanical properties at elevated temperatures are still lacking. Therefore, the aim of the present study was firstly to characterize the resulting microstructure of Al_2O_3-YAG-ZrO_2 composites fabricated by conventional ceramic processing with the ternary eutectic composition. And secondly, to assess their mechanical response at high temperatures by means of mechanical tests.

2 Experimental procedure

2.1 Material preparation

Samples of polycrystalline $Al_2O_3/Y_3Al_5O_{12}$(YAG)/Y_2O_3-stabilized ZrO_2(YSZ) with the eutectic composition were produced from commercial powders via a conventional solid-state reaction route. The starting powders were Al_2O_3 (Sigma-Aldrich, 99.99% purity), Y_2O_3 (Sigma-Aldrich, 99.999% purity), and 3 mol% Y_2O_3-stabilized ZrO_2 (Tosoh Corp., TZ-3Y-E grade, impurity content < 0.26 wt%). The powders were mixed in appropriate amounts to achieve the desired ternary eutectic composition (66 mol% Al_2O_3, 15 mol% Y_2O_3 and 19 mo% ZrO_2 [10]) and ball-milled in ethanol using agate media (grinding jar and 20-mm diameter balls) for 1 h. The powders were dried in air at 90 ºC for 24 h and then reground again using the same procedure as before to eliminate possible agglomerates. The resulting power mixture was uniaxial and isostatically pressed at room temperature at 150 and 210 MPa, respectively, into cylinders of 20 mm in diameter. Finally, the green pellets were sintered at 1500 ºC for 10 h in air, with heating and cooling ramps of 2 ºC/min. The density of the samples was determined using Archimedes' method. Sintered precursors obtained by a similar route were used to produce directionally-solidified ternary eutectic rods of about 2 mm in diameter (supplied by the Materials Science Institute of Aragón, Spain); a detailed description of the processing method can be found elsewhere [3]. The sintered rods were obtained by the laser-heated floating zone method using a CO_2 laser, at different growth rates between 25 and 750 mm/h.

The structural analysis of the crystalline phases in the sintered ceramic was performed on X-ray powder diffractograms obtained using a Bruker AXS D8 Advance X-ray diffractometer with Cu K_α radiation equipped with a scintillation detector in θ-2θ Bragg–Bentano configuration (X-ray Laboratory, CITIUS, University of Sevilla, Spain). A continuous scan mode was used to collect 2θ data from 10° to 120° in steps of 0.015° and a counting time of 0.5 s/step. X-ray tube voltage and current were set at 40 kV and 30 mA, respectively.

2.2 Microstructural observations

The microstructural characterization of both the as-fabricated and deformed material was carried out using scanning electron microscopy (SEM, Microscopy Service, CITIUS, University of Sevilla, Spain), mainly in the backscattered electron image mode. To this end, transverse and longitudinal (to the applied load direction in the case of deformed specimens) cross-sections were cut from the samples and mechanically polished using up to 0.5-μm grade diamond paste, and then thermally etched at 1200 ºC for 2 h in air. Elemental and compositional analysis was performed by energy dispersive X-Ray spectroscopy (EDS) to determine the different phases present in the material. The morphological parameters of these various phases were characterized by using a semiautomatic image analyzer.

2.3 Mechanical tests

Rectangular samples about 5 x 3 x 3 mm in size were cut from the sintered pellets with a low-

speed diamond saw and used for mechanical testing. Compression tests were carried out in air at temperatures T between 1200 and 1400 ºC. Two types of deformation tests were performed:
(i) at constant cross-head speed in a Microtest universal testing machine, at a nominal strain rate of $2x10^{-5}$ s^{-1}. The recorded data, load vs time t, were analyzed in $\sigma-\varepsilon$ curves, where ε is the true strain (= ln (l_o/l), with l_o and l the initial and instantaneous length, respectively) and σ is the true stress (= $\sigma_o$exp(-ε), with σ_o the initial stress); and
(ii) under constant load at nominal stresses between 40 and 60 MPa. In this case, the recorded experimental data, instantaneous specimen length l vs time t, were plotted as log $\dot{\varepsilon} - \varepsilon$ curves (usually called creep curves), where $\dot{\varepsilon} = d\varepsilon/dt$ is the strain rate. The load was applied gradually at the beginning of the tests.
Pads of SiC were inserted between the specimen and the alumina punching rams of the deformation machines to avoid, or at least to reduce, friction and indentation at the specimen-platen interfaces. The samples were typically deformed to total strains of 50-60% for subsequent microstructural observations, unless premature failure occurred.
The experimental data were analyzed using the standard high-temperature power law for steady-state deformation [11]:

$$\dot{\varepsilon} = A\sigma^{n}d^{-p}\exp(-Q/RT) \quad (1)$$

where A is a parameter depending on the deformation mechanism, d is the grain size, n is the stress exponent, p is the grain size exponent, Q is the activation energy for flow and R is the gas constant. The parameters n, p and Q are characteristics of the deformation mechanism [11]. In this work, stress and temperature changes were performed during a test on the same sample (differential method) in order to calculate the values of n and Q, respectively.

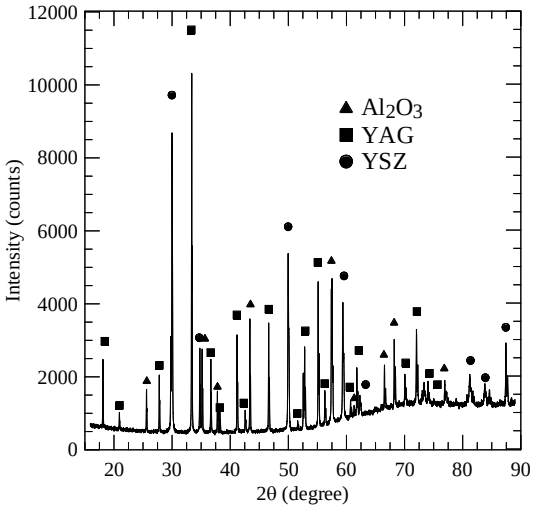

Figure 1. XRD pattern of polycrystalline Al_2O_3/YAG/YSZ with the eutectic composition. Peaks of monolithic Al_2O_3, YAG and YSZ phases are marked.

3 Results and discussion

Fig. 1 displays a XRD pattern of the as-received Al_2O_3/YAG/YSZ ternary composite. It shows that the material is formed by three phases, alumina, YAG and zirconia; every peak in the diffractogram can be assigned to one of these phases. Regarding the zirconia phase, the best fit with the experimental data was obtained with an yttria fully-stabilized cubic zirconia pattern. This is at variance with what has been reported recently by Oelgardt et al. [9] in

sintered Al_2O_3/YAG/YSZ polycrystals with the eutectic composition, where the zirconia phase after sintering was tetragonal. The difference may be due to the different sintering conditions between both studies: 1400 ºC and 1 h in Oelgardt's study, and 1500 ºC and 10 h in the present work. Matsui et al. [12] have reported the formation of cubic-phase regions with high Y^{3+} ion concentration in 3 mol% yttria-stabilized tetragonal zirconia (YTZP) after sintering at 1500 ºC for 2 h; the cubic phase started to form in grain interiors adjacent to the grain boundaries. At the sintering temperature of 1300 ºC, however, most of the grains were in the original tetragonal phase. Such a diffusive transformation phenomenon was termed grain boundary segregation-induced phase transformation. In directionally-solidified ternary eutectic Al_2O_3-YAG-ZrO_2 composites grown from the melt and processed from monoclinic zirconia, alumina and yttria powders, Oliete et al. [3] identified the zirconia phase as cubic zirconia, supporting the previous statement.

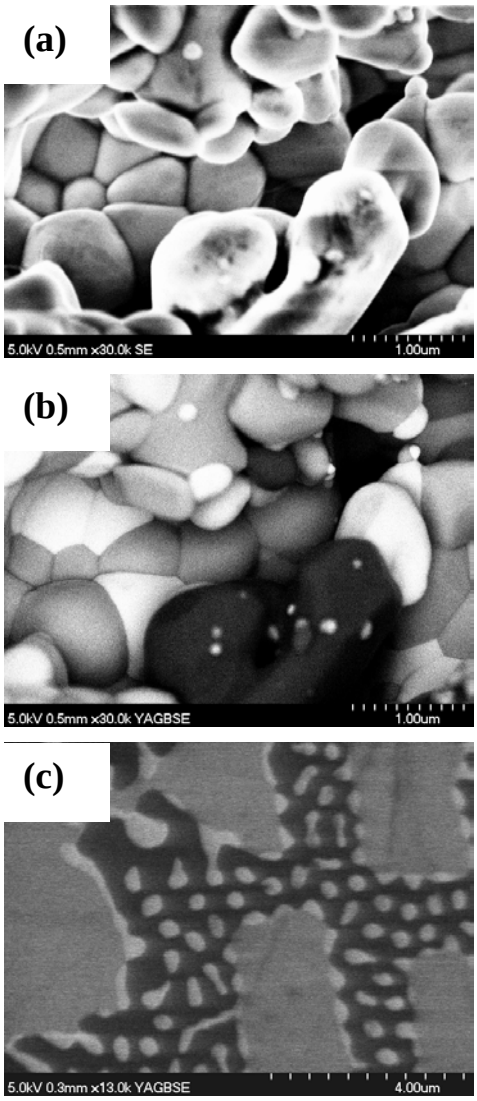

Figure 2. SEM micrographs of: Al_2O_3/YAG/ZrO_2 polycrystals in secondary (a) and backscattered (b) electron imaging mode; and directionally-solidified eutectic Al_2O_3/YAG/ZrO_2 (transverse cross-section, 25 mm/h) in backscattered mode (c). (Al_2O_3: black phase; YAG: gray; ZrO_2: white)

The microstructure of the as-received ceramic composite is depicted in Figs. 2a and 2b, which show representative SEM micrographs of polished and thermally-etched cross-sections of the material. The microstructure consists of equiaxed and fine grains (Fig. 2a), with an average grain size of about 0.5 μm. The three phases can be clearly distinguished in backscattered

electron imaging mode (Fig. 2b): Al_2O_3 (black phase), YAG (gray) and zirconia (white). This microstructure is very similar to that reported by Oelgardt et al. [9] in Al_2O_3-YAG-ZrO_2 eutectic-composition ceramic composites after sintering at 1500 ºC for 8 h.

The microstructure of the directionally solidified Al_2O_3-YAG-ZrO_2 eutectic oxide grown at 25 mm/h by the laser-heated floating zone is also shown for the sake of comparison (Fig. 2c). It is formed by a complex three-dimensional network of interpenetrating single crystal phases, without grain boundaries separating the individual phases. The interconnected phases form a Chinese script-like microstructure on transverse sections, which are elongated along the growth direction. The two majority phases, Al_2O_3 (dark) and YAG (gray), are faceted and have similar sizes. The zirconia phase appears more dispersed and smaller than the other two, forming short fibers (white) located within the Al_2O_3 phase and, to a lesser extent, at the Al_2O_3/YAG interfaces. The difference in morphology between the alumina and YAG phases, with irregular microstructures, and zirconia, with a regular microstructure formed by fibers, was ascribed to the different entropies of fusion of each phase. According to Hunt and Jackson theory [13], entropies of fusion higher than 2R, where R is the gas constant, produce faceted and irregular eutectic microstructures, whereas lower entropy values result in more regular rod/lamellae patterns, particularly at low growth rates. Alumina and the garnet have much higher entropies of melting than zirconia, thus resulting in a strong faceted growth of the majority phases and a rod-type morphology of the minority phase, as experimentally observed.

Regarding the mechanical behavior of the polycrystals, Fig. 3 displays the true stress σ – true strain curves at an initial strain rate of $2x10^{-5}$ s^{-1} as a function of the temperature between 1200 and 1400 ºC. There is a transition from brittle to ductile behavior as the temperature increases. At the lowest temperature studied, 1200 ºC, the sample exhibits a brittle behavior, failing catastrophically without plastic deformation after reaching a maximum stress of 240 MPa. At 1250 ºC, the specimen shows a semi-brittle behavior, failing after a plastic deformation of about 20%. At 1300 ºC, large deformations (> 50%) were achieved without macroscopic failure, though signs of degradation could be observed at strains higher than about 30% (the corresponding σ–ε curve exhibits softening at this strain). Finally, at 1350 and 1400 ºC, the compound exhibits extended steady states of deformation (secondary creep regime), characterized by a positive slope in the σ–ε plot due to the continuous decrease of the instantaneous specimen height (i.e., continuous increase of strain rate $\dot{\varepsilon}$) during compression. Concurrently there is a decrease in flow stress as the ductile behavior increases.

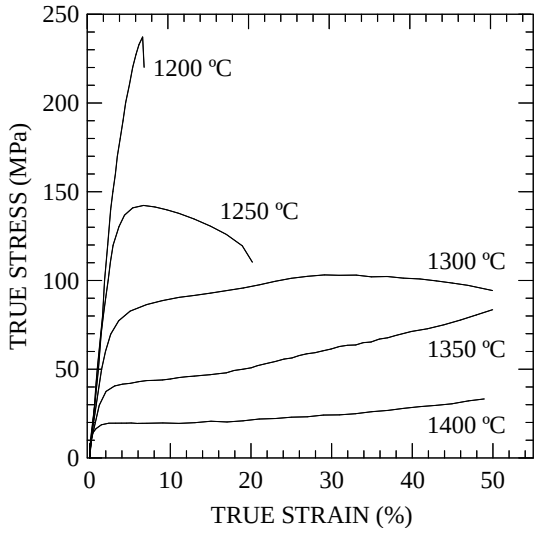

Figure 3. True stress vs true strain curves for polycrystalline Al_2O_3/YAG/YSZ as a function of the temperature for an initial strain rate of $2x10^{-5}$ s^{-1}.

In contrast, the σ–ε curves of directionally solidified AYZ eutectics grown from the melt deformed at 1400 ºC and similar initial strain rate [4] are characterized by a peak stress followed by flow softening, as could be expected from the absence of grain boundaries in the eutectic samples; no steady-state deformation was observed in any case.
The large strains attained in the ductile region indicate that grain boundary sliding is the main deformation mechanism, as found in other fine-grained superplastic metals and ceramics [14]. This conclusion is also suggested by the microstructure of the samples deformed under ductile conditions (Fig. 4), which appears almost featureless with respect to the undeformed ones.
In order to elucidate the deformation mechanisms operating in the composites at high temperatures, creep tests were performed at different loads and temperatures. Fig. 5 displays a representative log $\dot{\varepsilon}$ - ε curve obtained at 1350 ºC in air showing several determinations of the stress exponent n (Eq. (1)) by sudden up and down load changes during the test (differential method [11]). As can be seen, steady-state stages of deformation (secondary creep) were reached after each load change, characterized by a rather constant slope of the log $\dot{\varepsilon}$ - ε curve due to the continuous increase in sample cross-section, and subsequent stress reduction, with strain. The maintenance of the strain rate levels after the positive and negative load changes indicates that no microstructural evolution took place during deformation, in agreement with the microstructural observations.

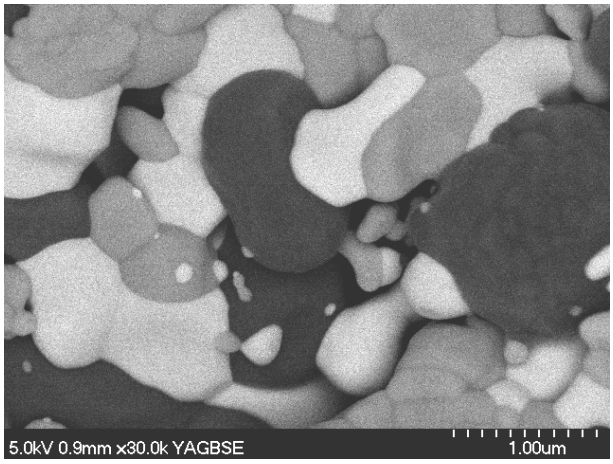

Figure 4. Microstructure of polycrystalline Al_2O_3/YAG/ZrO_2 deformed at 1350 °C up to a final strain of 50%. The stress axis is vertical

In such conditions, the stress exponent n can be easily deduced from the steady-state strain rates (Eq. (1)) before $\dot{\varepsilon}_1$ and after $\dot{\varepsilon}_2$ the stress change from σ_1 to σ_2:

$$n = \left.\frac{\log(\dot{\varepsilon}_2 / \dot{\varepsilon}_1)}{\log(\sigma_2 / \sigma_1)}\right|_{\varepsilon=cte} \qquad (2)$$

As depicted in Fig. 5, an average value n = 1.9 was measured. A value of 2 has been systematically reported in fine-grained superplastic ceramics and metals [14], where deformation is achieved by grain boundary sliding. It is also predicted by most theoretical models based on grain boundary sliding to explain superplasticity [14]. In this mechanism, the macroscopic deformation of the specimen is accommodated by the sliding of the grains over each other without appreciable deformation of the grains themselves, allowing very large strains (even several hundred per cent) to be achieved. The value of n = 1.9 experimentally

found by load changes agrees, therefore, with the absence of microstructural modifications observed in the strained samples with respect to undeformed ones.

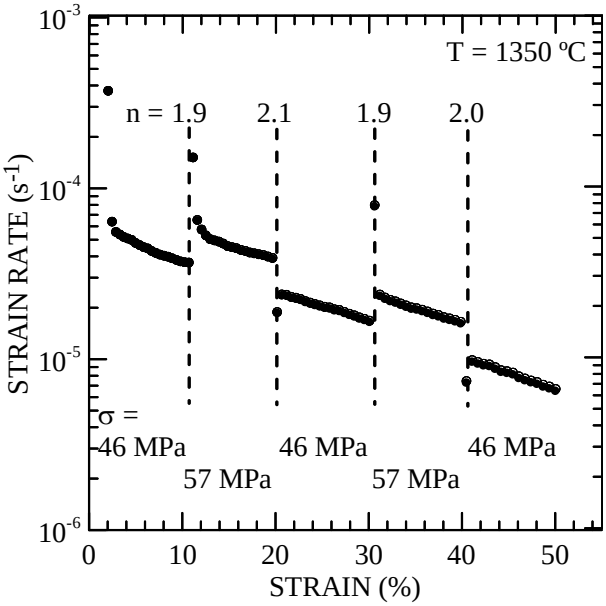

Figure 5. Creep curve of polycrystalline Al_2O_3/YAG/ZrO_2 deformed at 1350 ºC showing several determinations of the stress exponent n (Eq. (1)) by stress changes.

When plastic deformation is achieved by grain boundary sliding, diffusion is usually the rate-controlling mechanism [11,14]. The creep activation energy (Eq. 1) can be thus identified with the diffusion energy of the slowest moving species in the compound along the fastest path. A value of Q = 660 ± 40 kJ/mol has been determined from temperature changes in this work; the same value was estimated from constant strain rate experiments. Unfortunately, such a value is within the range of activation energies reported for alumina and YAG [14], precluding the exact determination of the strain-rate controlling phase.

4 Conclusions

Al_2O_3-$Y_3Al_5O_{12}$-ZrO_2 polycrystals with the ternary eutectic composition were prepared by solid-state reaction. After sintering at 1500 ºC for 10 h in air, the samples exhibit a homogeneous and very fine-grained microstructure of equiaxed grains with average size of 0.5 μm. The compound shows a high ductility above 1300ºC, without noticeable changes in grain shape and size even at strains of 50%. The apparent stress exponent measured from stress changes is close to 2. Microstructural observations and mechanical data are consistent with a superplastic behavior due to grain boundary sliding, as found in fine-grained superplastic metals and ceramics.

Acknowledgments

This work was supported by the Project nº MAT2009-13979-C03-01, Ministerio de Ciencia e Innovación, Spain.

References

[1] Lee J.H., Yoshikawa A., Murayama Y., Waku Y., Hanada S., Fukuda T. Microstructure and mechanical properties of Al_2O_3/$Y_3Al_5O_{12}$/ZrO_2 ternary eutectic materials. *J. Eur. Ceram. Soc.* **25**, 1411-1417 (2005).

[2] Pastor J.Y., Llorca J., Salazar A., Oliete P.B., de Francisco I., Peña J.I. Mechanical properties of melt-grown alumina–yttrium aluminum garnet eutectics up to 1900 K. *J. Am. Ceram. Soc*. **88**, 1488-1495 (2005).
[3] Oliete P.B., Peña J.I., Larrea A., Orera V.M., Llorca J., Pastor J.Y., Martín A., Segurado J. Ultra-high strength nanofibrillar Al_2O_3-YAG-YSZ eutectics. *Adv. Mater*. **19**, 2313-2318 (2007).
[4] Huamán-Mamani F.A, Jiménez-Melendo M., Mesa M.C., Oliete P.B. Microstructure and high-temperature mechanical behavior of melt-growth $Al_2O_3/Er_3Al_5O_{12}/ZrO_2$ ternary eutectic composites. *J. Alloys Compd*., in press (DOI:10.1016/j.jallcom.2012.01.105).
[5] Zhang J., Su H., Song K., Liu L., Fu H. Microstructure, growth mechanism and mechanical property of Al_2O_3-based eutectic ceramic in situ composites. *J. Eur. Ceram. Soc*. **31**, 1191-1198 (2011).
[6] French J.D., Chan H.M., Harmer M.P., Miller, G.A. High-temperature fracture toughness of duplex microstructures. *J. Am. Ceram. Soc*. **79**, 58-64 (1996).
[7] Flacher O., Blandin J.J., Plucknett K.P. Effects of zirconia additions on the superplasticity of alumina–zirconia composites. *Mater. Sci. Engng*. A221, 102-112 (1996).
[8] Jiménez-Melendo M., Haneda H., Nozawa H. Ytterbium cation diffusion in yttrium aluminum garnet (YAG) – Implications for creep mechanisms. *J. Am. Ceram. Soc*. **84**, 2356-2360 (2001).
[9] Oelgardt C., Anderson J., Heinrich J.G., Messing G.L. Sintering, microstructure and mechanical properties of Al_2O_3–Y_2O_3–ZrO_2 (AYZ) eutectic composition ceramic microcomposites. *J. Eur. Ceram. Soc*. **30**, 649-656 (2010).
[10] Lakiza S.A., Lopato L.M., Nazarenko L.V., Zaitseva A.A. The liquidus surface in the Al_2O_3–ZrO_2–Y_2O_3 phase diagram. *Powder Metall. Met. Ceram.* **33**, 595-598 (1994).
[11] Poirier J.P. *Creep of Crystals*. Cambridge University Press, Cambridge (1985).
[12] Matsui K., Horikoshi H., Ohmichi N., Ohgai1 M., Yoshida H., Ikuhara Y. Cubic-Formation and Grain-Growth Mechanisms in Tetragonal Zirconia Polycrystal. *J. Am. Ceram. Soc*. **86**, 1401-1408 (2003).
[13] Hunt J.D., Jackson K.A. Binary eutectic solidification. *Trans. Metall. Soc. AIME* **236**, 843-852 (1966).
[14] Nieh T.G., Wadsworth J., Sherby O.D. *Superplasticity in metals and ceramics*. Cambridge University Press, Cambridge (1997).